Pattern Recognition Letters
journal homepage: www.elsevier.com

Mutimodal ranking optimization for heterogeneous face re-identification

Hui Hu[a], Jiawei Zhang[a], Zhen Han[a]

[a] *Wuhan University, ..., ..., Wuhan, China*

arXiv:2212.05510v1 [cs.CV] 11 Dec 2022

Article history:

Keywords:
face re-identification
multimodal
re-ranking

ABSTRACT

Heterogeneous face re-identification, namely matching heterogeneous faces across disjoint visible light (VIS) and near-infrared (NIR) cameras, has become an important problem in video surveillance application. However, the large domain discrepancy between heterogeneous NIR-VIS faces makes the performance of face re-identification degraded dramatically. To solve this problem, a multimodal fusion ranking optimization algorithm for heterogeneous face re-identification is proposed in this paper. Firstly, we design a heterogeneous face translation network to obtain multimodal face pairs, including NIR-VIS/NIR-NIR/VIS-VIS face pairs, through mutual transformation between NIR-VIS faces. Secondly, we propose linear and non-linear fusion strategies to aggregate initial ranking lists of multimodal face pairs and acquire the optimized re-ranked list based on modal complementarity. The experimental results show that the proposed multimodal fusion ranking optimization algorithm can effectively utilize the complementarity and outperforms some relative methods on the SCface dataset.

© 2022 Elsevier Ltd. All rights reserved.

1. Introduction

Face re-identification, which refers to matching the same facial images across non-overlapping cameras, has become an emerging research area for security applications. Different from low-resolution face recognition, whose goal is to find the same person from a high-resolution face set given a low-resolution face image, face re-identification is to match the same person from two low-resolution face sets. The two image sets make the bidirectional ranking possible. In other words, after querying images of one set in the other set, we can use images of the result as new probes to query in the former set. Such differences make face re-identification methods significantly different from face recognition methods. Recently, as more and more near-infrared cameras are being installed, face re-identification is required to match between heterogeneous NIR and VIS face sets. In this scenario, the performance of traditional methods will degrade dramatically due to the large modality gap between NIR and VIS faces, which makes heterogeneous face re-identification a challenging problem.

Existing re-identification methods mainly focus on person re-identification, which refers to matching human bodies across disjoint cameras. In recent years, the re-ranking method, namely refining results by ranking the initial ranked lists again, is drawing more and more attention for its effectiveness in person re-identification. Some supervised re-ranking methods [1, 2, 3, 4] are proposed, that need either human intervention or label information. Recently, various unsupervised re-ranking methods [5, 6, 7, 8, 9, 10, 11] for person re-identification are proposed and have achieved excellent performance. However, these methods cannot be directly applied in heterogeneous face re-identification. This is because they only consider images in one modality, which causes difficulties in measuring pairwise similarity between VIS and NIR images and thus reduces the performance of the initial ranking and re-ranking. Re-ranking is also applied in face recognition, and some recent methods [12, 13, 14] have been proposed to deal with heterogeneous images. However, these methods also have limitations in face re-identification because face recognition has only one

e-mail: (Hui Hu), (Jiawei Zhang), (Zhen Han)

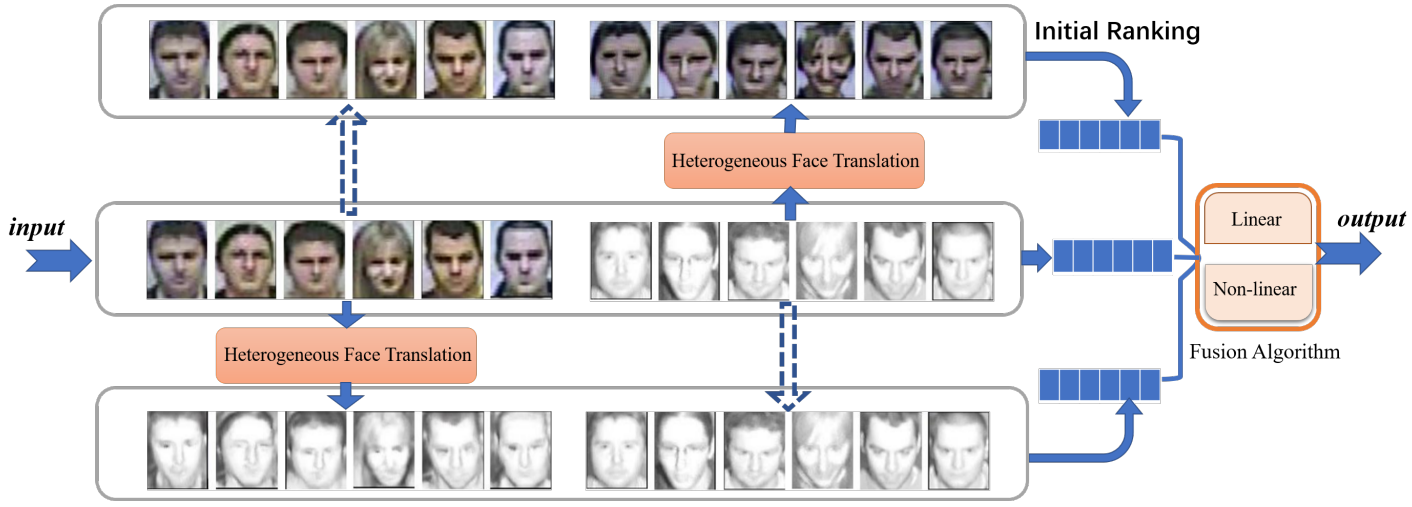

Fig. 1. Workflow

heterogeneous probe image that makes bidirectional ranking cannot be applied. Although person re-identification and heterogeneous face recognition are already widely discussed, heterogeneous face re-identification is still a relatively unexplored area, which contains both the ambiguity problem in person re-identification and the modality gap problem in face recognition.

In order to reduce the discrepancies between modalities, inspired by image-to-image translation, we intend to first convert heterogeneous images to homogeneous ones. Therefore, we design a bidirectional heterogeneous face translation network to convert the NIR images to fake VIS images and convert VIS images to fake NIR images. After the conversion, we obtain multimodal face pairs containing NIR (true)-NIR (fake), VIS (fake)-VIS (true), and original VIS (true)-NIR (true) on which the initial ranking process can be carried out separately. Then all initial ranking results are aggregated since we consider the multimodal face pairs have complementary information. This is because there are different biases lying in different modal pairs: On one hand, even though the converted fake NIR and VIS images are homogeneous, they are low-fidelity images. In this way, the ranking result calculated merely on VIS (fake)-VIS (true) or NIR (true)-NIR (fake) pairs are biased. On the other hand, though the original NIR (true)-VIS (true) pairs are high-fidelity, they have huge discrepancies between NIR and VIS which also leads to biased results. We consider that the different biases offered by different modal pairs provide complementary information in the ranking process. Therefore, a novel re-ranking algorithm has been proposed to fuse all biased initial ranking results and acquire an optimized ranking result.

Based on the ranking lists we obtained, the proposed fusion algorithm attempts to re-compute the distance between the probe image and each gallery image. The algorithm contains two individual parts. The first one is a linear fusion algorithm that simply takes the weighted sum of all results from different ranking lists. In order to define the weight of every result, we take the proportion of k-reciprocal neighbors in top-k nearest neighbors as an indication of confidence. The second method is a non-linear fusion algorithm that takes the minimal value of k as a new distance of the given probe image and gallery image which makes them the k-reciprocal neighbors. The final new distance which is then used for re-ranking can be obtained by aggregating results from the linear fusion algorithm and the non-linear fusion algorithm. The workflow is shown in Fig 1.

The main contributions of our work can be summarized as follows.

(1) The heterogeneous face translation network is designed to convert heterogeneous face images to homogeneous images, which can reduce the discrepancies between NIR and VIS modalities.

(2) The similarity-pushing and dissimilarity-pulling training strategy is proposed for the network to exploit more complementary information between modalities. Two kinds of complementarities are recognized and discussed in this paper.

(3) A multimodal fusion algorithm is proposed for the re-ranking process, which includes a linear fusion algorithm and a non-linear fusion algorithm. By using the obtained complementary information, the proposed method can further improve the initial ranking results.

2. Related work

Heterogeneous face re-identification is a relatively unexplored area. The two most related studies are person re-identification and heterogeneous face recognition.

re-ranking for person re-identification. In the past, person re-identification methods mainly focus on feature representations, feature transformations, and metric learning. Recently, various re-ranking methods are proposed and have shown great improvement. Bai et al. [15] propose

a sparse context activation method to express the similarity of samples and thus improve the ranking results. Jegou et al. [16] propose a context dissimilarity metric method that iteratively averages the distance from each point to its neighbors to define a new composite similarity. Qin et al. [17] firstly introduce the concept of k reciprocal nearest neighbors, which are considered high correlation candidates. Zhong et al. [18] utilize k reciprocal nearest neighbors to define a Jaccard distance, and then combine the Jaccard distance and initial distance as a new metric way. Bai et al. [19] propose a unified algorithm that combines existing fusion with diffusion strategies to exploit the complementarity of multiple metrics. Zhu et al [20] propose a feature relation map to mine the relationship between k nearest neighbors and utilize a similarity evaluation model to obtain the re-ranking results. However, because these methods are merely conducted on visible images, the performance will degrade significantly in heterogeneous scenarios due to the huge modality gap between VIS and NIR images. In recent years, some methods [21, 22] are proposed to deal with cross-modality person re-identification. However, these methods mainly focus on feature representations and do not utilize re-ranking for improvement.

re-ranking for heterogeneous face recognition. In recent years many re-ranking methods are also proposed for heterogeneous face recognition. Mudunuri et al. [12] propose an orthogonal dictionary alignment approach to learn the correspondence between two different domains and then re-rank the initial results by considering the similarity arrangement of the gallery data. Peng et al. [13] propose a high-dimensional deep local representation method to extract patch-level face features and use a locally linear re-ranking technique to re-rank initial results. Liu et al. [14] propose an iterative local re-ranking with an attribute-guided synthesis method. They first utilize the attribute-guided synthesis method to eliminate the face perception biases and then re-rank the initial results by integrating the local invariant information. However, face recognition is a different scenario from face re-identification where we have a set of heterogeneous face images rather than a single image. In addition, the low resolution of images makes face recognition methods difficult to be applied.

3. Method

In this section, we present the proposed method that consists of two stages: heterogeneous face image translation and multi-modal ranking optimization. We assume that $X = \{x1, x2, ...\}$ are VIS images and $Y = \{y1, y2, ...\}$ are NIR images. Our method first converts X and Y respectively and obtains several ranking lists. Then all ranking lists are aggregated by linear and non-linear re-ranking methods to obtain an optimized result. Each stage is described as follows.

3.1. Heterogeneous Face Image Translation

The main challenge in NIR and VIS matching is the modality gap. Motivated by [23], we propose to learn the modality gap by a bidirectional generative network. Given the X and Y, the network can convert x_i and y_j to $y_i^{'}$ and $x_j^{'}$ simultaneously, and finally obtain $X^{'} = \{x1^{'}, x2^{'}, ...\}$ and $Y^{'} = \{y_1^{'}, y_2^{'}, ...\}$. Thus, various ranking lists are obtained by comparing X with $X^{'}$, Y with $Y^{'}$, and X with Y. The three ranking lists are considered complementary and thus can be aggregated for re-ranking. However, such a simple conversion process suffers from the drawback that the generated $X^{'}$ and $Y^{'}$ have more biases since each image has only one generated low-fidelity result. To eliminate the biases, we propose the similarity pushing and dissimilarity pulling training strategy, which converts each image into two different images and thus provides more complementarities.

3.1.1. Similarity pushing and dissimilarity pulling training strategy

To eliminate the biases in generated images, instead of using a single translation network, we propose to use two different networks which are trained by positive samples and negative samples respectively. Here, positive samples refer to paired VIS and NIR samples, and negative samples refer to unpaired VIS and NIR samples. The illustration of the positive-sample trained network is shown in Fig 2. The positive sample trained network tries to make the gen-

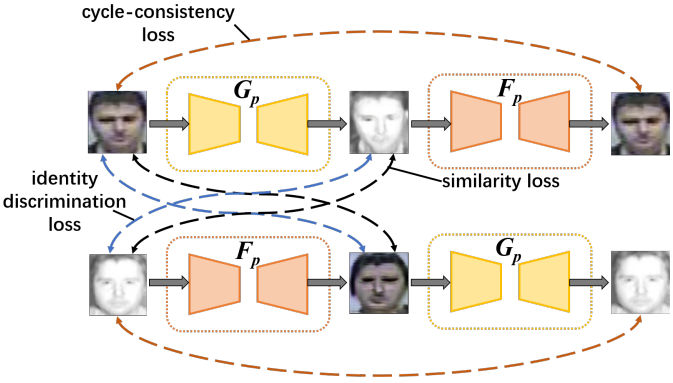

Fig. 2. Positive-sample Trained Network

erated image $x_i^{'}$ (or $y_i^{'}$) more similar to the corresponding true image x_i (or y_i), which we call similarity pushing. For this purpose, we introduce a positive sample similarity loss function:

$$L_p(f_1, f_2) = (1 - \frac{f_1 \cdot f_2}{|f_1| \cdot |f_2|})^2 \quad (1)$$

Here f_1 and f_2 represent face feature vectors extracted by the face feature extraction network. By minimizing $L_p(f_1, f_2)$, f_1 and f_2 will be much closer, thus the generated images will be much similar to the true images. The illustration of the negative sample trained network is shown in Fig 3. The negative sample trained network tries to make the generated image $x_j^{'}$ (or $y_i^{'}$) more dissimilar to the true image x_i (or y_j), which we call dissimilarity

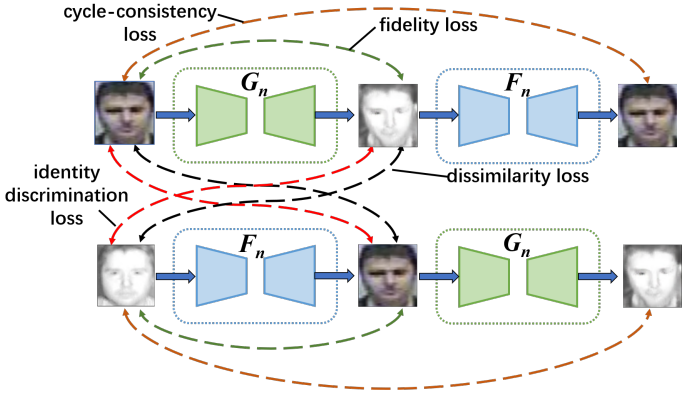

Fig. 3. Negative-sample Trained Network

pulling. For this purpose, we introduce a negative sample dissimilarity loss function:

$$L_n(f_1, f_2) = \{\max(0, \frac{f_1 \cdot f_2}{|f_1| \cdot |f_2|})\}^2 \quad (2)$$

By minimizing $L_n(f_1, f_2)$, the cosine value of f_1 and f_2 will decrease, and thus the generated $x_j^{'}$ (or $y_i^{'}$) will be more dissimilar to the true image x_i (or y_j). Here, we use the max function to constrain the dissimilarity pulling, since it can even make generated $x_j^{'}$ (or $y_i^{'}$) lose face features of y_j (or x_i). If the cosine value is greater than 0, the training process continues. Once the cosine value becomes less than 0, the training process stops. In addition, we also introduce a fidelity loss function, which is defined as the same as the positive sample similarity loss function Eq. (1) to further make sure the generated $x_j^{'}$ (or $y_i^{'}$) and the input y_j (or x_i) are of the same face. Finally, given the image sets X and Y, we can obtain 4 sets of generated images including $X_p^{'}$, $X_n^{'}$, $Y_p^{'}$, and $Y_n^{'}$, where p denotes that the set of images is generated by the positive-sample trained network and n denotes the set of images is generated by the negative-sample trained network. The initial ranking can be conducted on 5 set pairs: $Q_1 = \{X, Y\}$, $Q_2 = \{X, X_p^{'}\}$, $Q_3 = \{X, X_n^{'}\}$, $Q_4 = \{Y, Y_p^{'}\}$, and $Q_5 = \{Y, Y_n^{'}\}$.

3.1.2. Complementarity analysis

We consider these ranking lists are complementary and the complementary information can be categorized as inter-modality complementarity and intra-modality complementarity. The ranking lists obtained from Q_1, Q_2 (or Q_3), and Q_4 (or Q_5) are considered complementary since they are computed from different combinations of modalities. So we call it inter-modality complementarity. The ranking lists from Q_2 and Q_3 (or Q_4 and Q_5) are also considered complementary since the $X_p^{'}$ and $X_n^{'}$ (or $Y_p^{'}$ and $Y_n^{'}$) are generated from different networks, though they are in the same modality. So we call it intra-modality complementarity. We show the two types of complementarity in Fig 4.

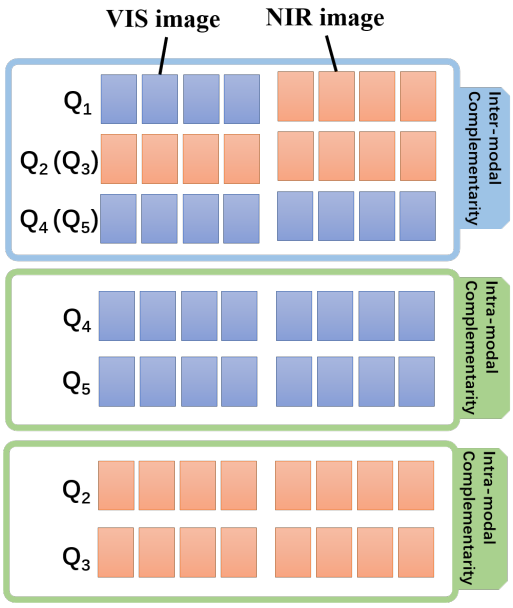

Fig. 4. Complementarities

3.2. Multimodal fusion algorithm

After the 5 set pairs are obtained, we conduct a bidirectional ranking method [24] as the initial ranking method, which includes a forward ranking that finds a probe image in the gallery set and a backward ranking that finds a gallery image in the probe set. As shown in Fig 5, given a probe p and a target g, the corresponding image of p and g in set pair Q_i is denoted as p^{Q_i} and g^{Q_i}. For every Q_i, we first find p^{Q_i} in the gallery set to obtain a forward ranking list, and then find g^{Q_i} in the probe set to obtain a backward ranking list. Therefore, for the p and g, there are 5 forward ranking lists and 5 backward ranking lists in total. The ranks of g in backward ranking lists and the ranks of

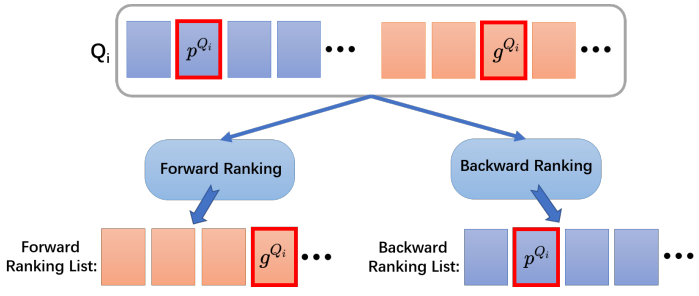

Fig. 5. Bidirectional Ranking

p in forward ranking lists are indications of the distance between g and p. In other words, g is more likely to be the correct match of p if g^{Q_i} ranks top in the forward ranking list of Q_i or p^{Q_i} ranks top in the backward ranking list of Q_i. In this way, given a probe p and a target g, we can fuse 10 ranks to define a new distance for re-ranking. The multimodal ranking optimization method which consists of a linear and a non-linear fusion algorithm is proposed for the fusion process. Each algorithm is described as follows.

3.2.1. Linear fusion algorithm

The linear fusion algorithm is to fuse 10 ranks using weighted sum, thus the main problem is how to assign different weights for each rank. Because it is known that the k-reciprocal neighbors of a probe image are more related to the probe image than the k nearest neighbors of it, we set greater the weight for an order if the more k-reciprocal neighbors are at the top-k images of the ranking list. For a probe p, we first define the k nearest neighbors as:

$$N(Q_i, p, k) = \{g_{p,1}^{Q_i}, g_{p,2}^{Q_i}, \ldots, g_{p,k}^{Q_i}\}, |N(Q_i, p, k)| = k \quad (3)$$

where k is a super-parameter and $|...|$ denotes the number of images in the set. Then, the k-reciprocal neighbors are defined as

$$R(Q_i, p, k) = \{g_{p,j} \mid (g_{p,j}^{Q_i} \in N(Q_i, p, k)) \wedge (p^{Q_i} \in N(Q_i, g_{p,j}, k))\} \quad (4)$$

The $R(Q_i, p, k)$ is a subset of k nearest neighbors of p^{Q_i} where p^{Q_i} is also of the k nearest neighbors of each image. We believe that the larger the number of images in $R(Q_i, p, k)$ is, the closer the k nearest neighbors are to the k- reciprocal neighbors, and subsequently, the more reliable the ranking list is. Hence, the weight for ranks from Q_i is defined as

$$W(Q_i, p, k) = \frac{|R(Q_i, p, k)|}{k} \quad (5)$$

We show an example when $k = 3$ in Fig 6. Given a probe

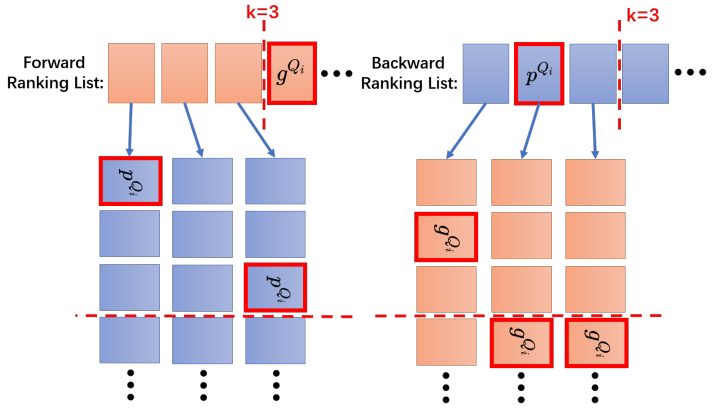

Fig. 6. Linear Fusion Algorithm

m and a target n, the new distance D_1 is described as

$$D_1(m, n) = \sum_{i=1}^{5} (W(Q_i, m, k) \cdot w \mid_{g_{m,w}^{Q_i} = n^{Q_i}} + W(Q_i, n, k) \cdot v \mid_{p_{n,v}^{Q_i} = m^{Q_i}}) \quad (6)$$

where v and w denote the ranks of m and n in Q_i.

3.2.2. Non-linear fusion algorithm

Different from the linear fusion algorithm, which takes the weighted sum of ranks from respective ranking lists according to the probability of fidelity, the non-linear fusion algorithm aims to choose a representative rank from all ranking lists as a new distance for re-ranking. When exploring the linear fusion algorithm, we observe that the minimal k which makes a probe p^{Q_i} and a target g^{Q_i} to be k-reciprocal neighbors is an indication of the distance between p and g. Suppose g^{Q_i} is the ith image in the forward ranking list and p is the jth image in the backward ranking list. When $k = \max(i, j)$, it becomes the minimal k that makes p^{Q_i} and g^{Q_i} to be k-reciprocal images. If p^{Q_i} is not similar with g^{Q_i}, the minimal k that makes p^{Q_i} and g^{Q_i} become k-reciprocal neighbors will be greater.

In the multimodal scenario, where there are 5 forward ranking lists and 5 backward ranking lists, we hope firstly aggregate ranks from forward and backward ranking lists respectively to obtain two possible ks, and then choose the greater one as the result. To aggregate the 5 forward

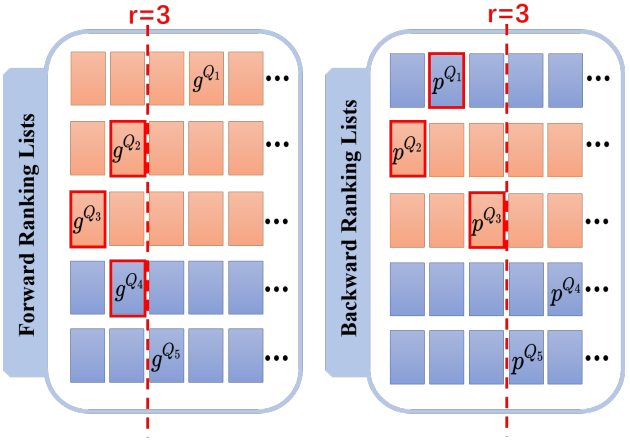

Fig. 7. Non-linear Fusion Algorithm

ranking lists and 5 backward ranking lists, we introduce r to choose the representative result. r is defined as the number of ranking lists where the target is at the top-k images. As shown in Fig 7, $r = 3$ indicates that there have to be at least 3 ranking lists where the target is at the top-k images. Based on the definition of $N(Q_i, m, k)$, we first define the multimodal k nearest neighbors as

$$\overline{N}(m, k, r) = \bigcup_{i_1 \neq i_2 \neq \cdots \neq i_r} (N(Q_{i_1}, m, k) \cap N(Q_{i_2}, m, k) \cap \cdots \cap N(Q_{ir}, m, k)) \quad (7)$$

Images in $\overline{N}(m, k, r)$ are images that rank top k in at least r ranking lists. Thus, the multimodal k-reciprocal neighbors are defined as

$$\overline{R}(m, k, r) = \{g_{m,j} \mid (g_{m,j} \in \overline{N}(m, k, r)) \wedge (m \in \overline{N}(g_{m,j}, k, r))\} \quad (8)$$

Images in $\overline{R}(m, k, r)$ are at the top-k results of at least r forward ranking lists, and at the same time, the probe image m are at the top-k results of at least r backward ranking lists. Our objective is to find a minimal k that

makes n belong to $\overline{R}(m,k,r)$. Considering the definition of $\overline{R}$, the k which makes n belongs to $\overline{R}(m,k,r)$ also makes n belongs to $\overline{N}(m,k,r)$ and makes m belong to $\overline{N}(n,k,r)$. Therefore, we can firstly compute a minimal k_1 that makes n belongs to $\overline{R}(m,k,r)$ and then compute a minimal k_2 that makes m belong to $\overline{R}(m,k,r)$. The final k is the greater one of k_1 and k_2. To compute the k_1, we can rank all ranks of n, and then the rth rank is the minimal k_1 that makes n at the top-k results of r ranking lists or more. Similarly, we can rank all ranks of m and take the rth rank as k_2. The distance between a probe m and a target n can be described as

$$D_2(m,n) = \max(\min k_1 \mid_{n\in\overline{N}(m,k_1,r)}, \min k_2 \mid_{m\in\overline{N}(n,k_2,r)}) \tag{9}$$

3.3. Full fusion function

Given a probe m and a target n, the new distance for re-ranking can be defined as the fusion of results from the linear fusion algorithm and non-linear fusion algorithm, which is described as

$$D(m,n) = \lambda \cdot D_1 + (1-\lambda)\cdot D_2 \tag{10}$$

where λ is used to control the relative importance of the linear fusion algorithm and non-linear fusion algorithm.

4. Experiments

In this section, the performance of the proposed method will be evaluated on the SCface [25] dataset which contains face images from both NIR and VIS. The results and analysis of our experiment are as follows.

4.1. Experiment Details

dataset. In this paper, we choose the publicly available SCface dataset, because images from most other public heterogeneous facial datasets (like PolyU or CASIA NIR-VIS) are relatively high-resolution and do not have variations in pose, which is not consistent with a practical video surveillance scenario. The SCface dataset contains 4160 static images of 130 subjects from both the NIR and VIS spectra. Each subject is photographed at different ranges and degrees leading to different image resolutions and pose variations. Here, we select 1 low-resolution NIR image and 1 low-resolution VIS image per subject and there are 130 pairs of NIR and VIS images, and then split them into two subsets of 65 pairs each. Each subset contains 35 pairs for training and 30 pairs for testing. Examples of two subsets are shown in Fig 8.

evaluation metric. For performance evaluation, all experimental results are shown in the Cumulative Matching Characteristics (CMC) curve. The CMC curve is a plot of the recognition performance versus the rank score and represents the expectation of finding the correct match within the top k matches. For each method, we report its CMC@1, CMC@5, and CMC@10.

Fig. 8. Subsets of the SCface Dataset

implementation. We use Arcface and Sphereface for feature extraction. For Arcface, we resize all images to the resolution of 122*122 to fit the input size of Arcface; for Sphereface, we resize them to the resolution of 112*96 to fit the input size of Sphereface. Each experiment is conducted in Arcface and Sphereface separately. As for the parameters of our method, λ_1 and λ_2 are set to 0.25 and 0.75 by default. We use Adam optimizer at recommended parameters with an initial learning rate of 0.0002. The training epoch is 200.

4.2. Comparison Experiment

We compare our method with three related re-ranking algorithms: attribute-guided re-ranking [14], dictionary alignment re-ranking [12], and k-reciprocal encoding [18]. The CMC curves show that our method achieves higher performance than all three methods and has a large improvement on initial results. We report the average CMC@1, CMC@5, and CMC@10 accuracies on two subsets in Table 1. As shown in Table 1, our method achieves higher accuracy than initial ranking results both in CMC@1, CMC@5, and CMC@10 accuracies. However, the results from all the other methods are even lower than the initial ranking results. This is because: For the proposed method, our heterogeneous face translation network fully exploits complementarities and then the multimodal re-ranking algorithm refines results by linear and nonlinear fusion algorithms. For the iterative local re-ranking with the attribute-guided synthesis method, the low resolution of the images makes the face attributes ambiguous, thus the attribute-guided

Table 1. Average CMC of Different Methods on Two Subsets

Method	Rank1	Rank5	Rank10
Baseline [1]	38.96%	55%	66.16%
k-reciprocal [18]	24.15%	31.45%	37.9%
Attribute guided [14]	28.43%	37.66%	48.06%
Dictionary alignment [12]	37.22%	51%	63.3%
our method	50.63%	66.26%	75.84%

[1] Only conduct forward ranking on initial VIS and NIR images

synthesis introduces more biases and leads to the degradation of the re-ranking method. For the re-ranking with dictionary alignment, the performance of face alignment degrades due to the low resolution and the lack of details, thus more biases of similarity arrangement in initial rank lists are introduced, which leads to the low accuracy of final results. In addition, both re-ranking with attribute-guided synthesis and re-ranking with dictionary alignment consider only one heterogeneous probe image without exploiting the relationship between the probe image and other images of the same modality.

4.3. Ablation Study

Table 2. Average CMC of Similarity Pushing and Dissimilarity Pulling Ablation Study on Two Subsets

Method	Rank1	Rank5	Rank10
Baseline	38.96%	55%	66.16%
Baseline + 1[1]	46.26%	62.3%	71.8%
Baseline + 2[2]	48.33%	64.36%	75.41%
Baseline + 1 + 2	50.63%	66.26%	75.84%

[1] Conduct dissmilarity pulling strategy
[2] Conduct similarity pushing strategy

Table 3. Average CMC of Linear and Non-Linear Fusion Algorithm Ablation Study on Two Subsets

Method	Rank1	Rank5	Rank10
Baseline	38.96%	55%	66.16%
Baseline + 1[1]	43.13%	68.13%	77.49%
Baseline + 2[2]	35.83%	64.39%	73.13%
Baseline + 1 + 2	50.63%	66.26%	75.84%

[1] Conduct linear fusion algorithm
[2] Conduct non-linear fusion algorithm

In this subsection, we evaluate the effectiveness of each component of the proposed method. First, the effectiveness of the similarity pushing and dissimilarity pulling strategy is shown in Table 2. Regardless of forward or backward ranking, both similarity pushing and dissimilarity pulling can improve accuracies, and similarity pushing + dissimilarity pulling is more likely to further improve the accuracies. Then, the effectiveness of linear and nonlinear fusion algorithms is shown in Table 3. It shows that both linear and nonlinear fusion algorism are more likely to gain increases in CMC@5 and CMC@10. The accuracies of CMC@1 are improved little or even drop. However, the aggregated results of linear and nonlinear fusion algorithms can gain increases in all CMC@1, CMC@5, and CMC@10.

5. Conclusion

In this work, we proposed a multimodal face ranking optimization algorithm to address the heterogeneous face re-identification problem. A heterogeneous face image translation network is designed to learn the modality gap between heterogeneous images and the similarity pushing and dissimilarity pulling strategy is adopted to exploit the complementary information. Besides, a multimodal fusion algorithm, which consists of a linear fusion algorithm and a non-linear fusion algorithm is proposed to re-rank the results by using the complementary information to fuse different ranking results. Experiments show the effectiveness of the proposed method on face re-identification. Because existing NIR-VIS face databases are collected for face recognition which does not take some factors like pose variation and occlusion into account, one of the future works is to collect a more reliable face image database for heterogeneous face re-identification.

References

[1] C. Liu, C. C. Loy, S. Gong, G. Wang, Pop: Person re-identification post-rank optimisation, in: Proceedings of the IEEE International Conference on Computer Vision, 2013, pp. 441–448.

[2] S. Bai, X. Bai, Q. Tian, Scalable person re-identification on supervised smoothed manifold, in: Proceedings of the IEEE Conference on Computer Vision and Pattern Recognition, 2017, pp. 2530–2539.

[3] H. Wang, S. Gong, X. Zhu, T. Xiang, Human-in-the-loop person re-identification, in: European conference on computer vision, Springer, 2016, pp. 405–422.

[4] J. Jia, Q. Ruan, Y. Jin, G. An, S. Ge, View-specific subspace learning and re-ranking for semi-supervised person re-identification, Pattern Recognition 108 (2020) 107568.

[5] M. Ye, C. Liang, Z. Wang, Q. Leng, J. Chen, Ranking optimization for person re-identification via similarity and dissimilarity, in: Proceedings of the 23rd ACM international conference on Multimedia, 2015, pp. 1239–1242.

[6] J. Garcia, N. Martinel, C. Micheloni, A. Gardel, Person re-identification ranking optimisation by discriminant context information analysis, in: Proceedings of the IEEE International Conference on Computer Vision, 2015, pp. 1305–1313.

[7] M. Ye, J. Chen, Q. Leng, C. Liang, Z. Wang, K. Sun, Coupled-view based ranking optimization for person re-identification, in: International Conference on Multimedia Modeling, Springer, 2015, pp. 105–117.

[8] L. Jiang, C. Liang, D. Xu, W. Huang, Multi-similarity re-ranking for person re-identification, in: 2019 IEEE International Conference on Image Processing (ICIP), IEEE, 2019, pp. 1212–1216.

[9] J. Lv, Z. Li, K. Nai, Y. Chen, J. Yuan, Person re-identification with expanded neighborhoods distance re-ranking, Image and Vision Computing 95 (2020) 103875.

[10] Y. Zhang, Q. Qian, C. Liu, W. Chen, F. Wang, H. Li, R. Jin, Graph convolution for re-ranking in person re-identification, in: ICASSP 2022-2022 IEEE International Conference on Acoustics, Speech and Signal Processing (ICASSP), IEEE, 2022, pp. 2704–2708.

[11] M. Hanif, H. Ling, W. Tian, Y. Shi, M. Rauf, Re-ranking person re-identification using distance aggregation of k-nearest neighbors hierarchical tree, Multimedia Tools and Applications 80 (5) (2021) 8015–8038.

[12] S. P. Mudunuri, S. Venkataramanan, S. Biswas, Dictionary alignment with re-ranking for low-resolution nir-vis face recognition, IEEE Transactions on Information Forensics and Security 14 (4) (2018) 886–896.

[13] C. Peng, N. Wang, J. Li, X. Gao, Re-ranking high-dimensional deep local representation for nir-vis face recognition, IEEE Transactions on Image Processing 28 (9) (2019) 4553–4565.

[14] D. Liu, X. Gao, N. Wang, C. Peng, J. Li, Iterative local re-ranking with attribute guided synthesis for face sketch recognition, Pattern Recognition 109 (2021) 107579.

[15] S. Bai, X. Bai, Sparse contextual activation for efficient visual re-ranking, IEEE Transactions on Image Processing 25 (3) (2016) 1056–1069.

[16] H. Jegou, H. Harzallah, C. Schmid, A contextual dissimilarity measure for accurate and efficient image search, in: 2007 IEEE Conference on computer vision and pattern recognition, IEEE, 2007, pp. 1–8.

[17] D. Qin, S. Gammeter, L. Bossard, T. Quack, L. Van Gool, Hello neighbor: Accurate object retrieval with k-reciprocal nearest neighbors, in: CVPR 2011, IEEE, 2011, pp. 777–784.

[18] Z. Zhong, L. Zheng, D. Cao, S. Li, Re-ranking person re-identification with k-reciprocal encoding, in: Proceedings of the IEEE conference on computer vision and pattern recognition, 2017, pp. 1318–1327.

[19] S. Bai, P. Tang, P. H. Torr, L. J. Latecki, Re-ranking via metric fusion for object retrieval and person re-identification, in: Proceedings of the IEEE/CVF Conference on Computer Vision and Pattern Recognition, 2019, pp. 740–749.

[20] B. Zhu, T. Xu, B. Zheng, Q. Zhang, Y. Sun, A. Liu, Z. Mao, C. Yan, Evolution of icts-empowered-identification: A general re-ranking method for person re-identification, Pattern Recognition Letters 150 (2021) 94–100.

[21] M. Ye, X. Lan, Z. Wang, P. C. Yuen, Bi-directional center-constrained top-ranking for visible thermal person re-identification, IEEE Transactions on Information Forensics and Security 15 (2019) 407–419.

[22] Y. Feng, J. Xu, Y.-m. Ji, F. Wu, Llm: Learning cross-modality person re-identification via low-rank local matching, IEEE Signal Processing Letters 28 (2021) 1789–1793.

[23] J.-Y. Zhu, T. Park, P. Isola, A. A. Efros, Unpaired image-to-image translation using cycle-consistent adversarial networks, in: Proceedings of the IEEE international conference on computer vision, 2017, pp. 2223–2232.

[24] Q. Leng, R. Hu, C. Liang, Y. Wang, J. Chen, Bidirectional ranking for person re-identification, in: 2013 IEEE International Conference on Multimedia and Expo (ICME), IEEE, 2013, pp. 1–6.

[25] M. Grgic, K. Delac, S. Grgic, Scface–surveillance cameras face database, Multimedia tools and applications 51 (3) (2011) 863–879.